Heliyon 9 (2023) e12962

Contents lists available at ScienceDirect

Heliyon

journal homepage: www.cell.com/heliyon

Research article

Chemical reaction, Dufour and Soret effects on the stability of magnetohydrodynamic blood flow conveying magnetic nanoparticle in presence of thermal radiation: A biomedical application

Cédric Gervais Njingang Ketchate [a,*], Pascalin Tiam Kapen [b,c,**], Inesse Madiebie-Lambou [c], Didier Fokwa [a], Victorin Chegnimonhan [d,e], René Tchinda [b,c], Ghislain Tchuen [b,c]

[a] Laboratory of Mechanics, University of Douala, Douala, Cameroon
[b] URISIE, University Institute of Technology Fotso Victor, University of Dschang, P.O Box 134, Bandjoun, Cameroon
[c] UR2MSP, Department of Physics, University of Dschang, P.O Box 67, Dschang, Cameroon
[d] Centre Béninois de la Recherche Scientifique et l'Innovation, Cotonou, Benin
[e] Laboratoire de Thermique et Energie de Nantes, UMR 6607, CNRS, Nantes, France

ARTICLE INFO

Keywords:
Chemical reaction
Dufour effect
Soret effect
Ferrofluid
Stabilty analysis

ABSTRACT

Nowadays ferrofluids (magnetic nanofluids) are at the center of many researches because of their major biomedical applications such as drug delivery and cancer treatment. The effects of chemical reaction, temperature gradient induced mass transfer and concentration gradient induced heat transfer on the stability of ferrofluid flow are of great importance. This paper deals with a stability analysis of a ferrofluid composed of blood as base fluid and magnetic nanoparticles. The study integrates the effects of chemical reactions, the effects of mass transfer (Soret effect), the effects of heat transfer (Dufour effect) and the effects of the Buoyancy force. The flow is exposed to a magnetic field and thermal radiation. A system of eigenvalue equations governing the evolution of disturbances is derived by assuming a normal mode analysis. This system of equations is then solved numerically by the method of collocation. It appears from this study that the addition of nanoparticles to the blood increases its inertia, which dampens the amplitude of the disturbances and stabilizes the flow. The Casson parameter affects the stability of the flow by increasing the amplitude of the disturbances, which reflects its destabilizing effect. It appears from this study that taking into account the non-Newtonian nature of blood is very important when modeling the dynamics of the system because it shows more important and very different results than when blood is treated as a Newtonian fluid. The chemical reaction between the fluid and the nanoparticles leads to the redistribution of disturbances within the flow, which amplifies the instabilities and reflects the destabilizing character of the chemical reaction. On the other hand, temperature gradient induced mass transfer effects and concentration gradient induced heat transfer effects play an essential role on the stability of the flow because they attenuate the amplitude of the disturbances in the flow. The Darcy number exhibits a stabilizing effect on the flow. It appears from this analysis that the porosity of the medium increases the contact surface

* Corresponding author.
** Corresponding author. URISIE, University Institute of Technology Fotso Victor, University of Dschang, P.O Box 134, Bandjoun, Cameroon.
E-mail addresses: cketchate@gmail.com (C.G. Njingang Ketchate), fpascalin20022003@yahoo.fr (P. Tiam Kapen).

https://doi.org/10.1016/j.heliyon.2023.e12962
Received 28 July 2022; Received in revised form 29 December 2022; Accepted 10 January 2023
Available online 16 January 2023

between the fluid and the nanoparticles. Buoyancy forces, thermal radiation parameter and wave number contribute to the stability of the flow. The magnetic field through the Lorentz force decreases the kinetic energy of the flow, which dissipates the disturbances and thus reflects the stabilizing character of the magnetic field. It should be noted that heat and mass transfer on magnetohydrodynamic flows through porous media taking into consideration the effect of chemical reaction appears in many natural and artificial transport processes in several branches of science and engineering applications. This phenomenon plays an important role in the chemical industry, power and cooling industry for drying, chemical vapor deposition on surfaces, cooling of nuclear reactors and petroleum industry. The effects of thermal radiation, mass and heat transfer are used in many situations in biomedical engineering and aerospace engineering.

Nomenclature

u, v	Velocity component
x, y	Cartesian coordinates
t	Time
C_p	specific heat capacity
B	Magnetic field
B_0	Applied magnetic field
E	Electric field
T	Temperature
T_∞	Fluid temperature in the free stream
T_1, T_2	Temperature at the wall
k	Thermal conductivity
g	Gravity acceleration
k	Permeability of the medium
q_r	Radiative heat flux
M	Hartmann number
R_d	Radiation parameter
P_r	Prandtl number
D_a	Darcy number
S_C	Schmidt number
S_r	Soret number
D_u	Dufour number
R_i	Richardson number
N	Buoyancy parameter
R_e	Reynold's number
P	Pressure
D_m	Mass diffusion ration,
K_T	Thermal diffusion ration,
C_s	Concentration susceptibility,
k_0	Chemical reaction parameter,
J	Current density vector,
C	Speed of disturbances
U	Mean velocity
K_c	Chemical reaction parameter
A, B	Matrices
a_n, b_n, c_n	Chebyshev coefficients
I	Identity matrice
T_i	Chebyshev polynomial

Greek symbols

β_T	Thermal expansion coefficient
β_c	The mass transfer expansion
α	Wave number
Φ	Concentration

Φ_1, Φ_2	Concentration at the wall
μ	Dynamic viscosity
β	Thermal expansion coefficient
ρ	Density
σ	Electrical conductivity
(βC_p)	Heat capacitance
φ	Volume fraction of magnetic nanoparticle
σ^*	Stefan-Boltzmann constant
θ	Dimensionless temperature
β_R	Absorption coefficient
μ_0	Magnetic permeability of emptiness
ε_0	Permissiveness of emptiness

Sub scripts

s	Solid nanoparticles
f	Base fluid
nf	Nanoliquid
hnf	Hybrid nanoliquid

1. Introduction

Nowadays, the therapeutic treatment of diseases is based on the targeted administration of drugs using magnetic nanoparticles in the human cardiovascular system. Widder and Senyer were the first scientists to put forward the idea of using magnetic nanoparticles to deliver drugs to a patient. In this therapeutic treatment technique, magnetic nanoparticles and drug molecules are injected into the blood and are transported to the target organs using magnetic fields which are generally applied locally and facilitate the release of drugs encapsulated by the magnetic nanoparticles. This technique is used in several biomedical applications such as the treatment of cancer, the transport of drugs by targeted administration, the treatment of wounds, separation of blood cells, reduction of bleeding during surgical operations and also the magnetization of blood. It should be noted that the set consisting of blood and magnetic nanoparticles forms a new category of fluid called nanofluid [1]. A nanofluid is a composition of nanoparticles of nanometric size suspended in a base fluid. In the literature, we find several types of nanoparticles, namely silver, copper, alumina, iron, aluminum oxide, titanium oxide, iron oxide, gold, single wall carbon nanotube, multi wall carbon nanotube etc [2,3]. As base fluid, mention may be made of water, blood, glycol, ethylene, etc. Thus several types of nanofluid exist thus depending on the type of nanoparticle used or on the type of base fluid chosen. Nanofluids have applications in the field of medicine, in renewable energy systems, transport, chemical manufacturing, automobiles, solar collector, nuclear reactor, industrial cooling, solar synthesis, gas sensing, bio-sensing, petroleum engineering, thermal engineering etc [4,5]. These dispersed nanoparticles significantly improve the thermal conductivity of the nanofluid and improve the coefficients of conduction and convection taking into account greater heat transport. Recent developments in technology necessitate an innovative revolution in the field of heat transfer. Researchers on nanofluids have been amplified rapidly and reports have revealed that nanofluids are advantageous heat transfer fluids for engineering and manufacturing and biomedical applications.

The flow of blood carrying magnetic nanoparticles through blood vessels is similar to a problem of fluid flow in pipes and is in fact a problem of fluid mechanics. Like any fluid flow, the dynamics can evolve and pass from a laminar flow to a turbulent flow. The laminar-turbulent transition is caused by the birth and growth of instabilities. The origin of instabilities may be due to gravity, surface tension, a difference in density within the flow or even a significant production of kinetic energy during the flow. In most practical cases, it is necessary and very important to control the flow, which justifies the interest of such a study.

Magnetohydrodynamics (MHD) is the part of fluid mechanics that deals with the dynamics of electrically conductive fluids such as blood, electrolytes and metallic liquids in the presence of the magnetic field. MHD has applications in medicine, MHD generators, MHD pumps, chemical engineering, electrostatic filter, petroleum engineering [6–8].

Theoretically, the magnetic field acts on a moving electrically conductive fluid through the Lorentz force which generally slows the motion of the fluid and increases the temperature and concentration of the fluid. In the literature, there are several works related to MHD. Kapen et al. [2] showed the stabilizing effects of the magnetic field on a flow of hybrid nanofluid. Khashi'ie et al. [9] presented the effects of the magnetic field on a hybrid nanofluid boundary layer over a stretching/shrinking sheet. Their study also takes Joule effects into account. Kapen et al. [10] carried out a study based on a linear stability analysis of blood flow with iron oxide nanoparticles. It emerges from their study that the magnetic field impacts the flow by contributing to the stability of the suspension. Zainal et al. [11] investigated MHD nanofluid convection with convective boundary conditions. Their results show that the magnetic field increases the speed of the flow. Lanjwani et al. [12] performed MHD boundary layer stability of nanofluid flow treated as Casson's fluid. He observed a double solution during their studies, the first of which is stable.

When density differences within a fluid are important, the Soret and Dufour effects should not be neglected. The Soret effect translates in fact a mass transfer within a flow created by a temperature gradient and the Dufour effect represents a heat transfer within a flow created by a concentration gradient. The combined effects of heat and mass transfer have contributions in thermal insulation,

compact heat exchangers, paper production, catalytic reactor, separation of isotopes and in the mixture of gases of different molar mass [13]. Sheikholeslami et al. [14] studied the thermal diffusion and heat generation effects on the unsteady MHD flow of radiating and electrically conducting nanofluid past over an oscillating vertical plate through porous medium. The effects of Soret and Dufour number on convective boundary layer flow have been examined by Ahmma and Krishna [15]. Umavathi and Chamkha [16] presented a stability analysis of a nanofluid flow in a porous channel taking into account the Soret and Dufour effects. Their work shows that the Dufour and Soret effects help stabilize the flow. Maiti et al. [17] showed that Dufour effects have an impact on the growth of the Nusselt number. Bég et al. [18] showed the Soret and Dufour effects on natural convection from a spherical body. Mishra et al. [19] presented the Soret effect on the micropolar fluid on a streching sheet with hydromagnetic effects. Mittal [20] discussed heat and mass transfer of nanofluid flow through two horizontal parallel plates in a rotating system subject to magnetic field effects. Postelnicu [21] explored the effects of Soret and Dufour on heat and mass transfer. Chamkha and Rashad [22] highlighted in their work the effects of the chemical reaction and the magnetic field, of Soret and of Dufour on the stability of the convective mixed flow on a vertical cone. Other works on the Soret and Dufour effects are available in the following literature [23–25].

The chemical reaction results from an interaction between one or more bodies which produce one or more new bodies. Many chemical reactions require heat or a catalyst to occur. A distinction is made between homogeneous chemical reactions and heterogeneous chemical reactions. A homogeneous chemical reaction is a reaction in which the reactants and the catalyst are in the same phase. Whereas a heterogeneous reaction is a reaction for which the reactants and the catalyst are not in the same phase.

Umavathi and Chamkha [16] during the analysis of the stability of the convective flow of nanofluid in porous channel showed that the chemical reactions affect the stability of the flow and have a destabilizing effect. Maiti et al. [17] showed that chemical reactions increased wall shear stress. The same effect of the chemical reaction was observed by Mekheimer et al. [26] when analyzing the stability of Jeffrey's nanofluid flow. Krishna et al. [27] showed the effects of the chemical reaction, the Hall effect, the effects of ionic sliding on the MHD convection of microplastic fluid on a porous plate. Other works integrating the effects of chemical reactions on flow dynamics are available in the following literature [28, 29].

In most flow applications, the treated fluids are non-Newtonian fluids. These classes of fluid have attracted the attention of physicists, engineers and mathematicians. Non-Newtonian fluids have applications in medicine, chemical industry, biotechnology etc. The mathematical modeling of non-Newtonian fluids is based on non-linear behavior laws which generally links stress rates to strain rates. In the literature several mathematical models exist to represent the dynamics and mechanisms of heat transport in non-Newtonian fluids. Among the various mathematical models, we have Casson's modeling which is widely accepted. Casson's fluids have applications in fields such as biomedical and industrial engineering, power generation, mechanics and geophysical fluid dynamics. A casson's fluid is a fluid that exhibits an elastic limit. If a stress is applied which is lower than the elastic limit, the fluid does not flow and behaves like a solid. On the other hand, if the stress applied is greater than the elastic limit, the fluid flows [30,31]. Thus, Casson's fluid exhibits zero viscosity at infinite shear rate and infinite viscosity at zero shear rate. Examples of casson fluid include human blood, tomato sauce, honey, biological fluids, jelly, honey. Krishna et al. [30] explored the unsteady radiative magnetohydrodynamic (MHD) flow on a porous surface in vertical motion. Their results showed that velocity increased with thermal buoyancy and concentration forces. Rasool et al. [32] discussed the characteristics of non-Newtonian nanofluid flowing through an absorbent medium past a nonlinear stretching surface with a view to enhancing mass and heat transport. A numerical study of Casson's nanofluid on a parallel stretching surface with hydromagnetic and Joule heating effects with slip and thermal convection boundary condition was presented by Kamran et al. [33]. Mousavi et al. [34] investigated the effect of Casson's model for stable laminar MHD hybrid nanofluid flow due to sheet stretching/shrinking with effects of suction, radiation and convective boundary conditions. Dual solutions to the problem were also considered. Hamid [35] studied the mixed convection of a two-dimensional flow of non-Newtonian nanofluids in the presence of thermal radiation and heat source/sink effects.

The scrutinize of thermal radiation in heterogeneous areas in engineering such as nuclear power plants, multifarious propulsion devices for missiles, liquid metal fluids, gas turbines and so forth, due to small coefficient of convective heat transfer, demonstrates the surface heat transfer. Thermal radiation is distinguished in numerous applications because of the perspective in which radiant emission relies on temperature. The unstable MHD boundary layer of nanofluid flowing over a moving vertical surface incorporating the phenomenon of thermal radiation absorption have been explored by Krishna et al. [36]. Their study shows that Radiation-absorbed parameter plays a prominent role in enhancing the velocity as well as the temperature in the boundary layer region. Ketchate et al. [37] investigated a linear stability analysis of mixed convection of a Newtonian nanofluid flow through a porous channel exposed to thermal radiation transverse to the flow direction. Their result shows that the thermal radiation parameter affects the stability of the flow and has a stabilizing effect. Sobamowo [38] studied the heat transfer effects of thermal radiation on free convection flow of Casson nanofluid over a vertical plate. Ahmmed et al. [39] discussed the unstable MHD free convection flow of a nanofluid through an exponentially accelerated tilted plate embedded in a porous medium with variable thermal conductivity in the presence of radiation.

Most problems involve the heat, mass, and momentum transfer processes that take place with chemical reactions. Based on these observations, an analysis of the flow stability of treated blood as a casson fluid transporting magnetic nanoparticles through a porous artery and integrating hydromagnetic and thermal radiation effects has not yet been investigated. Therefore, the effects of Soret, Dufour for mass and heat transfer and chemical reactions on the stability of the flow have been examined in detail by the existence of thermal radiation and the magnetic field. This investigation is organized as follows: Section 2 presents the mathematical modeling of the problem followed by section 3 which is reserved for an analysis of linear stability. Section 4 and section 5 respectively present the numerical method for solving the equations governing the stability of the flow and the results resulting from this numerical resolution. Finally, the conclusion is presented in the final section.

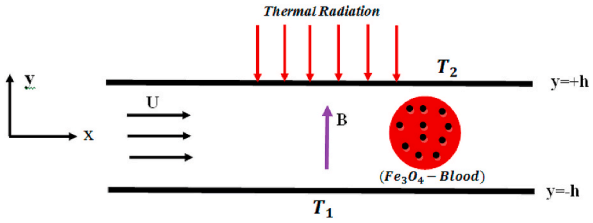

Fig. 1. Geometry of the problem.

2. Mathematical formulation of the problem

The present study focuses on the flow of blood modeled as Casson's fluid through a 1D rigid artery. Blood flow is placed under the influence of a uniform magnetic field perpendicular to the direction of flow and is also exposed to thermal radiation. The effects of mass diffusion being very important the effects of Dufour and Soret are taken into consideration. As a hypothesis, blood is treated as a viscous and incompressible fluid, flowing at low magnetic Reynolds number. The flow through the considered artery transports the magnetic nanoparticles whose distribution within the flow is uniform and homogeneous. No external electric field is applied such that the effect of polarization of fluid is negligible. A radiative heat flux q_r is applied in the normal direction to the flow.

Under the above assumptions, master equations (1)–(1)–(9)(1)–(9) such as continuity, Navier-Stokes, energy, concentration [2,17] and Maxwell equation [6] that govern the dynamics shown in Fig. 1 are.

$$\nabla \vec{V} = 0 \tag{1}$$

$$\rho_{nf}\frac{d\vec{V}}{dt} = -\nabla P + \mu_{nf}\left(1+\frac{1}{\beta}\right)\Delta\vec{V} - \mu_{nf}\frac{\vec{V}}{k} + \vec{J}\Lambda\vec{B} + (\rho\beta_T)_{nf}(T-T_1)\vec{g} + (\rho\beta_C)_{nf}(\Phi-\Phi_1)\vec{g} \tag{2}$$

$$(\rho C_P)_{nf}\frac{dT}{dt} = k_{nf}\Delta T + \frac{D_m K_T \rho_{nf}}{C_s}\Delta\Phi - \frac{\partial q_r}{\partial y} \tag{3}$$

$$\frac{d\Phi}{dt} = D_m\Delta\Phi + \frac{D_m K_T}{T_m}\Delta T - k_0(\Phi-\Phi_1) \tag{4}$$

$$\nabla\Lambda\vec{B} = \mu_0\left(\vec{J} + \varepsilon_0\frac{\partial\vec{E}}{\partial t}\right) \tag{5}$$

$$\nabla\Lambda\vec{E} = -\frac{\partial\vec{B}}{\partial t} \tag{6}$$

$$\nabla.\vec{B} = 0 \tag{7}$$

$$\nabla.\vec{E} = 0 \tag{8}$$

$$\nabla.\vec{J} = 0 \tag{9}$$

$$\vec{J} = \sigma_{nf}\left(\vec{E} + \vec{V}\Lambda\vec{B}\right) \tag{10}$$

The thermophysical parameters of the nanofluid are defined using Brinkman's model [40–42].

$$\rho_{nf} = (1-\varphi)\rho_f + \varphi\rho_s \tag{11}$$

$$\mu_{nf} = \mu_f(1-\varphi)^{-2.5} \tag{12}$$

$$\sigma_{nf} = \left[\frac{(1+2\varphi)\sigma_s + 2(1-\varphi)\sigma_f}{(1-\varphi)\sigma_s + (2+\varphi)\sigma_f}\right]\sigma_f \tag{13}$$

$$k_{nf} = \left[\frac{(k_s+2k_f) - 2(k_f-k_s)\varphi}{(k_s+2k_f) + (k_f-k_s)\varphi}\right]k_f \tag{14}$$

$$(\rho\beta)_{nf} = (1-\varphi)(\rho\beta)_f + (\rho\beta)_s\varphi \tag{15}$$

$$(\rho C_P)_{nf} = (1-\varphi)(\rho C_P)_f + (\rho C_P)_s \varphi \tag{16}$$

The radiative flux is expressed as follows through the Rooseland approximation [43,44].

$$q_r = -\frac{4\sigma}{3\beta_R}\frac{\partial T^4}{\partial y} \tag{17}$$

For small temperature differences within the flow [37], T can be decomposed into Taylor series as follows (18) [37]:

$$T^4 = 4T_\infty^3 T - 3T_\infty^3 \tag{18}$$

Thus, equation (17) becomes:

$$q_r = -\frac{16\sigma T_\infty^3}{3\beta_R}\frac{\partial T}{\partial y} \tag{19}$$

The equations governing the problem in Cartesian coordinates are (20–24) [2,17,37]:

$$\frac{\partial u}{\partial x} + \frac{\partial v}{\partial y} = 0 \tag{20}$$

$$\rho_{nf}\left(\frac{\partial u}{\partial t} + u\frac{\partial u}{\partial x} + v\frac{\partial u}{\partial y}\right) = -\frac{\partial p}{\partial x} + \mu_{nf}\left(1+\frac{1}{\beta}\right)\Delta u - \mu_{nf}\frac{u}{k} - \sigma_{nf}B_0^2 u \tag{21}$$

$$\rho_{nf}\left(\frac{\partial v}{\partial t} + u\frac{\partial v}{\partial x} + v\frac{\partial v}{\partial y}\right) = -\frac{\partial p}{\partial y} + \mu_{nf}\left(1+\frac{1}{\beta}\right)\Delta v - \mu_{nf}\frac{v}{k} + g(\rho\beta_T)_{nf}(T-T_1) + g(\rho\beta_c)_{nf}(\Phi-\Phi_1) \tag{22}$$

$$(\rho C_P)_{nf}\left(\frac{\partial T}{\partial t} + u\frac{\partial T}{\partial x} + v\frac{\partial T}{\partial y}\right) = k_{nf}\Delta T + \frac{\rho_{nf}D_m K_T}{C_s}\Delta\Phi + \frac{16\sigma T_\infty^3}{3\beta_R}\frac{\partial^2 T}{\partial y^2} \tag{23}$$

$$\left(\frac{\partial \Phi}{\partial t} + u\frac{\partial \Phi}{\partial x} + v\frac{\partial \Phi}{\partial y}\right) = D_m\Delta\Phi + \frac{D_m K_T}{T_m}\Delta T - k_0(\Phi-\Phi_1) \tag{24}$$

The boundary conditions of the problem shown in Fig. 1 [17]:

$$u = v = 0, T = 0, \Phi = 0 \text{ at } t = 0 \text{ for all } y \tag{24a}$$

$$u = v = 0, T = T_1, \Phi = \Phi_1, t \succ 0 \text{ at } y = -h \tag{24b}$$

$$u = v = 0, T = T_2, \Phi = \Phi_2, t \succ 0 \text{ at } y = +h \tag{24c}$$

To ease the manipulation of the equations, we can introduce the dimensionless parameters [2,37] below:

$$\widetilde{x} = \frac{x}{h}, \widetilde{y} = \frac{y}{h}, \widetilde{u} = \frac{u}{U}, \widetilde{v} = \frac{v}{U}, \widetilde{t} = t\frac{U}{h}, \widetilde{p} = \frac{p}{\rho_f U^2}, \widetilde{\theta} = \frac{T-T_1}{T_2-T_1}, \widetilde{\Phi} = \frac{\Phi-\Phi_1}{\Phi_2-\Phi_1} \tag{25}$$

By means of equation (25), we obtain the following equations (26-(26-30)(26-30):

$$\frac{\partial \widetilde{u}}{\partial \widetilde{x}} + \frac{\partial \widetilde{v}}{\partial \widetilde{y}} = 0 \tag{26}$$

$$\frac{\partial \widetilde{u}}{\partial \widetilde{t}} + \widetilde{u}\frac{\partial \widetilde{u}}{\partial \widetilde{x}} + \widetilde{v}\frac{\partial \widetilde{u}}{\partial \widetilde{y}} = -\frac{1}{f_s}\frac{\partial \widetilde{p}}{\partial \widetilde{x}} + \frac{\beta_1}{f_{\mathrm{Re}}R_e}\Delta\widetilde{u} - \frac{\widetilde{u}}{f_{\mathrm{Re}}D_a\mathrm{R}_e} - \frac{M^2}{f_M R_e}\widetilde{u} \tag{27}$$

$$\frac{\partial \widetilde{v}}{\partial \widetilde{t}} + \widetilde{u}\frac{\partial \widetilde{v}}{\partial \widetilde{x}} + \widetilde{v}\frac{\partial \widetilde{v}}{\partial \widetilde{y}} = -\frac{1}{f_s}\frac{\partial \widetilde{p}}{\partial \widetilde{y}} + \frac{\beta_1}{f_{\mathrm{Re}}R_e}\Delta\widetilde{v} - \frac{\widetilde{v}}{f_{\mathrm{Re}}D_a R_e} + f_{Ri}R_i\widetilde{\theta} + f_N N\widetilde{\Phi} \tag{28}$$

$$\left(\frac{\partial \widetilde{\theta}}{\partial \widetilde{t}} + \widetilde{u}\frac{\partial \widetilde{\theta}}{\partial \widetilde{x}} + \widetilde{v}\frac{\partial \widetilde{\theta}}{\partial \widetilde{y}}\right) = \frac{\Delta\widetilde{\theta}}{f_{\mathrm{Pr}}P_r R_e} + \frac{D_u}{f_{Du}R_e}\Delta\widetilde{\Phi} + \frac{R_d}{f_{Rd}P_r R_e}\frac{\partial^2\widetilde{\theta}}{\partial y^2} \tag{29}$$

$$\left(\frac{\partial \widetilde{\Phi}}{\partial \widetilde{t}} + \widetilde{u}\frac{\partial \widetilde{\Phi}}{\partial \widetilde{x}} + \widetilde{v}\frac{\partial \widetilde{\Phi}}{\partial \widetilde{y}}\right) = \frac{\Delta\widetilde{\Phi}}{R_e S_c} + \frac{S_r}{R_e}\Delta\widetilde{\theta} - K_c R_e\widetilde{\Phi} \tag{30}$$

The non-dimensional boundary conditions are (30a-30c) [17,37]:

$$\widetilde{u} = \widetilde{v} = 0, \widetilde{\theta} = 0, \widetilde{\Phi} = 0 \text{ at } t = 0 \text{ for all } y \tag{30a}$$

$$\widetilde{u}=\widetilde{v}=0,\widetilde{\theta}=0,\widetilde{\Phi}=0,t\succ 0 \text{ at } y=-1 \tag{30b}$$

$\widetilde{u}=\widetilde{v}=0,\widetilde{\theta}=1,\widetilde{\Phi}=1,t\succ 0$ at $y=+1$ (30c) R_e is Reynolds number [2], D_a is Darcy number [2], M is Hartmann's number [2], R_i is Richarson's (thermal buoyancy parameter) [37], N is buoyancy ratio parameter [17], D_u is Dufour's number, S_c is Schmidt's number [17], P_r is the Prandlt number [17], R_d is the thermal radiation parameter [37], S_r is the Soret number [17] and K_c is the chemical reaction parameter [16,17] defined as follow:

$$R_e=\frac{\rho_f hU}{\mu_f},M=B_0h\sqrt{\frac{\sigma_h}{\mu_f}},\beta_1=1+\frac{1}{\beta},R_i=\frac{g\beta_T(T_2-T_1)h}{U^2},N=\frac{g\beta_c(\Phi_2-\Phi_1)h}{U^2} \tag{31}$$

$$D_u=\frac{D_mK_T(\Phi_2-\Phi_1)}{C_s\upsilon_f(T_2-T_1)C_P},R_d=\frac{16\sigma T_\infty^3}{3\beta_Rk_f},P_r=\frac{\mu_f}{\rho_f\alpha_f},S_c=\frac{\upsilon_f}{D_m},K_c=\frac{k_0\upsilon_f}{U^2},S_r=\frac{D_mK_T(T_2-T_1)}{\upsilon_fT_\infty(\Phi_2-\Phi_1)} \tag{32}$$

Where, f_{Re}, f_M, f_s, f_{Ri}, f_N, f_{Pr}, f_{Du}, f_{Rd} denote adjustment factors defined as follows (33–34) [2,3]:

$$f_s=\frac{\rho_{nf}}{\rho_f},f_{\mathrm{Re}}=\frac{\rho_{nf}}{\rho_f}\frac{\mu_f}{\mu_{nf}},f_M=\frac{\rho_{nf}}{\rho_f}\frac{\sigma_f}{\sigma_{nf}},f_{\mathrm{Pr}}=\frac{(\rho C_P)_{nf}}{(\rho C_P)_f}\frac{k_f}{k_{nf}},f_{Rd}=\frac{(\rho C_P)_{nf}}{(\rho C_P)_f} \tag{33}$$

$$f_{Ri}=\frac{(\rho\beta_T)_{nf}}{(\rho\beta_T)_f}\frac{\rho_f}{\rho_{nf}},f_N=\frac{(\rho\beta_C)_{nf}}{(\rho\beta_C)_f}\frac{\rho_f}{\rho_{nf}},f_{Du}=\frac{(\rho C_P)_{nf}}{(\rho C_P)_f}\frac{\rho_f}{\rho_{nf}} \tag{34}$$

3. Linear stability analysis

For a linear stability analysis the solutions of equations (26-(26-30)(26-30) are sought in the form:

$$\begin{cases}\widetilde{u}(x,y,t)=U(y)+u(x,y,t)\\ \widetilde{v}(x,y,t)=v(x,y,t)\\ \widetilde{p}(x,y,t)=P(x)+p(x,y,t)\\ \widetilde{\theta}(x,y,t)=\overline{\theta}(y)+\theta(x,y,t)\\ \widetilde{\Phi}(x,y,t)=\overline{\Phi}(y)+\Phi(x,y,t)\end{cases} \tag{35}$$

Equation (35) shows a decomposition of the flow into base flow and disturbed flow. By means of equation (35), the following disturbance evolution equations emerge (36–40) [2,17]:

$$\frac{\partial u}{\partial x}+\frac{\partial v}{\partial y}=0 \tag{36}$$

$$\frac{\partial u}{\partial t}+U\frac{\partial u}{\partial x}+v\frac{\partial U}{\partial y}=-\frac{1}{f_s}\frac{\partial p}{\partial x}+\frac{\beta_1}{f_{\mathrm{Re}}R_e}\Delta u-\frac{u}{f_{\mathrm{Re}}D_aR_e}-\frac{M^2}{f_MR_e}u \tag{37}$$

$$\frac{\partial v}{\partial t}+U\frac{\partial v}{\partial x}=-\frac{1}{f_s}\frac{\partial p}{\partial y}+\frac{\beta_1}{f_{\mathrm{Re}}R_e}\Delta v-\frac{v}{f_{\mathrm{Re}}D_aR_e}+f_{Ri}R_i\theta+f_NN\Phi \tag{38}$$

$$\frac{\partial\theta}{\partial t}+U\frac{\partial\theta}{\partial x}+v\frac{\partial\overline{\theta}}{\partial y}=\frac{\Delta\theta}{f_{\mathrm{Pr}}P_rR_e}+\frac{D_u}{f_{Du}R_e}\Delta\Phi+\frac{R_d}{f_{Rd}P_rR_e}\frac{\partial^2\theta}{\partial y^2} \tag{39}$$

$$\frac{\partial\Phi}{\partial t}+U\frac{\partial\Phi}{\partial x}+v\frac{\partial\overline{\Phi}}{\partial y}=\frac{\Delta\Phi}{R_eS_c}+\frac{S_r}{R_e}\Delta\theta-K_cR_e\Phi \tag{40}$$

The divergence of the perturbation equations [2] gives (41):

$$\Delta p=\frac{M^2f_s}{R_ef_M}\frac{\partial v}{\partial y}+f_sf_{Ri}R_i\frac{\partial\theta}{\partial y}+f_sf_N\frac{\partial\Phi}{\partial y}-2f_s\frac{dU}{dy}\frac{\partial v}{\partial x} \tag{41}$$

The Laplacian of equation (38) gives

$$\left(\frac{\partial}{\partial t}+U\frac{\partial}{\partial x}+\frac{1}{f_{\mathrm{Re}}D_aR_e}-\frac{\beta_1}{f_{\mathrm{Re}}R_e}\Delta\right)\Delta v=\frac{d^2U}{dy^2}\frac{\partial v}{\partial x}-\frac{M^2}{f_MR_e}\frac{\partial^2v}{\partial y^2}+f_{Ri}R_i\left(\Delta\theta-\frac{\partial^2\theta}{\partial y^2}\right)+f_NN\left(\Delta\Phi-\frac{\partial^2\Phi}{\partial y^2}\right) \tag{42}$$

The stability analysis carried out in this study is based on an analysis in normal mode, thus the solution of equations (38, 40 and 42) is sought in the following form (43) [2,36]:

$$(v,\theta,\Phi)(x,y,t)=(\widehat{v},\widehat{\theta},\widehat{\Phi})(y)e^{i\alpha(x-ct)} \tag{43}$$

$\widehat{v},\widehat{\theta},\widehat{\Phi}$ are respectively the amplitudes of the velocity, temperature and concentration disturbances.

α is the wave number, C is the propagation speed of disturbances which in a stability analysis is complex and has the following form (44) [2]:

$$C = C_r + iC_i \tag{44}$$

The real part of equation (42) represents the propagation speed of the disturbances and the imaginary part is the rate of amplification of the disturbances. When this imaginary part is positive ($C_i > 0$), the disturbances propagate while increasing and the flow is unstable, when this imaginary part is negative ($C_i < 0$) the disturbances evolve while attenuating and the flow is stable and finally when this imaginary part is zero ($C_i = 0$), the disturbances propagate without amplification or attenuation and the flow is neutral.

Thus, (43) in equations (39), (40) and (42) gives:

$$\left[(U-C)\left(D^2-\alpha^2\right) - \frac{i\left(D^2-\alpha^2\right)}{\alpha f_{\mathrm{Re}} D_a R_e} + i\frac{\beta_1}{\alpha f_{\mathrm{Re}} R_e}\left(D^2-\alpha^2\right)^2\right]\widehat{v} = \frac{d^2U}{dy^2}\widehat{v} + i\frac{M^2}{\alpha f_M R_e}D^2\widehat{v} + i\alpha f_{Ri} R_i \widehat{\theta} + i\alpha f_N N \widehat{\Phi} \tag{45}$$

$$\left[(U-C) + \frac{i}{\alpha f_{\mathrm{Pr}} P_r R_e}\left(D^2-\alpha^2\right) + i\frac{R_d}{\alpha f_{Rd} P_r R_e}D^2\right]\widehat{\theta} = \frac{i}{\alpha}\frac{d\overline{\theta}}{dy}\widehat{v} - i\frac{D_u}{\alpha f_{Du} R_e}\left(D^2-\alpha^2\right)\widehat{\Phi} \tag{46}$$

$$\left[(U-C) - \frac{i}{\alpha}K_c R_e + \frac{i}{\alpha S_c R_e}\left(D^2-\alpha^2\right)\right]\widehat{\Phi} = \frac{i}{\alpha}\frac{d\overline{\Phi}}{dy}\widehat{v} - i\frac{S_r}{\alpha R_e}\left(D^2-\alpha^2\right)\widehat{\theta} \tag{47}$$

Equations (45-(45-47)(45-47) form a system of eigenvalue equations with which are associated the following boundary conditions (48) [40]:

$$\begin{cases} \widehat{v}'(-1) = \widehat{v}'(1) = 0 \\ \widehat{v}(-1) = \widehat{v}(1) = 0 \\ \widehat{\theta}'(-1) = \widehat{\theta}'(1) = 0 \\ \widehat{\Phi}'(-1) = \widehat{\Phi}'(1) = 0 \end{cases} \tag{48}$$

Equations (45-(45-47)(45-47) and boundary conditions (48) form the equations governing the disturbance dynamics. These equations do not admit analytical solutions but can be solved by an appropriate numerical method. Thus the numerical resolution of these equations will be made in the next section.

4. Numerical approach

This section presents the numerical resolution of the stability equations. This numerical resolution is based on Chebyshev's spectral collocation method [2,3,45]. The idea of this method is to search for unknown functions $\widehat{v}$, $\widehat{\theta}$ and $\widehat{\Psi}$ in the following form (49) [2,17]:

$$\widehat{v}(y) = \sum_{n=0}^{N} a_n T_n(y), \widehat{\theta}(y) = \sum_{n=0}^{N} b_n T_n(y), \widehat{\psi}(y) = \sum_{n=0}^{N} c_n T_n(y) \tag{49}$$

T_n is the Chebyshev polynomials defined by$T_n(\cos\theta) = \cos n\theta$. a_n, b_n and c_n are the Chebyshev coefficients.

Substituting the expression (49) in the stability equations (45-(45-47)(45-47) results in the following generalized eigenvalue problem (50) [17]:

$$A\psi = CB\psi \tag{50}$$

Where $\psi = (a_0, \ldots, a_N, b_0, \ldots, b_N, c_0, \ldots c_N)$, A and B are $3(N+1) \times 3(N+1)$ matrices defined as follows (51) [17]:

$$A = \begin{bmatrix} A_{11} & A_{12} & A_{13} \\ A_{21} & A_{22} & A_{23} \\ A_{31} & A_{32} & A_{33} \end{bmatrix} \text{ and} B = \begin{bmatrix} B_{11} & 0 & 0 \\ 0 & B_{22} & 0 \\ 0 & 0 & B_{33} \end{bmatrix} \tag{51}$$

A_{11}, A_{12}, A_{13}, A_{21}, A_{22}, A_{23}, A_{31}, A_{32}, A_{33}, B_{11}, B_{22}, B_{33} are block matrices of size $(N+1) \times (N+1)$ defined by (52-(52-55)(52-55) [17]:

$$A_{11} = U\left(D^2-\alpha^2 I\right) - i\frac{\left(D^2-\alpha^2 I\right)}{\alpha f_{\mathrm{Re}} D_a R_e} + i\frac{\beta_1}{\alpha f_{\mathrm{Re}} R_e}\left(D^2-\alpha^2 I\right)^2 - \frac{d^2U}{dy^2}I - i\frac{M^2}{\alpha f_M R_e}D^2 A_{12} = -i\alpha f_{Ri} R_i I \tag{52}$$

$$A_{13} = -i\alpha f_N N I, A_{21} = -\frac{i}{\alpha}\frac{d\overline{\theta}}{dy}I, A_{22} = UI + \frac{i}{\alpha f_{\mathrm{Pr}} P_r R_e}\left(D^2-\alpha^2 I\right) + \frac{iR_d}{\alpha f_{Rd} P_r R_e}D^2 \tag{53}$$

$$A_{23} = i\frac{D_u}{\alpha f_{Du} R_e}\left(D^2-\alpha^2 I\right), A_{31} = -\frac{i}{\alpha}\frac{d\overline{\Phi}}{dy}I, A_{32} = i\frac{S_r}{\alpha R_e}\left(D^2-\alpha^2 I\right) \tag{54}$$

Table 1
Properties of blood and magnetic nanoparticle [36].

	$\rho\ (kg.m^{-3})$	$C_p(J.kg^{-1}K^{-1})$	$K\ (w.\ m^{-1}K^{-1})$	$\sigma\ (S.m^{-1})$	$\beta\times 10^{-5}(K^{-1})$
Blood	1050	3617	0.52	0.8	0.18
Fe_3O_4	5200	670	9.7	25,000	1.3

$$A_{33} = UI - \frac{i}{\alpha}K_c R_e I + \frac{i}{\alpha S_c R_e}\left(D^2 - \alpha^2 I\right), B_{11} = D^2 - \alpha^2 I, B_{22} = B_{33} = I \tag{55}$$

The boundary conditions become (56) [17]:

$$\begin{cases} a_0 = a_N = 0 \\ \sum_{n=0}^{N} D_{0n} a_n = 0 \\ \sum_{n=0}^{N} D_{Nn} a_n \\ b_0 = b_N = 0 \\ c_0 = c_N = 0 \end{cases} \tag{56}$$

5. Results and discussion

This section is reserved for the presentation of the results obtained from the numerical resolution of the aforementioned equations. Table 1 below presents the physical properties of blood and the magnetic nanoparticle. On the different figures that will be presented, the yellow line is just there to separate the zone of stability from the zone of instability. The eigenvalues of the system of equations were calculated using Matlab software. To verify our numerical scheme, we have shown in Fig. 2 the variation in the rate of amplification of the disturbances as a function of the Reynolds number. We have made the approximation of a flow without nanoparticles and in the absence of various effects such as the magnetic field, the thermal radiation, the Dufour and Soret effects, the chemical reactions and the porosity of the medium. The model in Fig. 1 is therefore reduced to the flow model studied by Makinde [46]. It is observed through this figure that the critical Reynolds number corresponding to a critical wave number a = 1.02 for which there is transition to instabilities is Rec = 5772.17. This value of the Reynolds critical number is in agreement with those obtained by Makinde [46].

Fig. 3 presents the effects of the presence of magnetic nanoparticles on the stability of the flow. This figure shows that for $\alpha = 1$ and $\alpha = 1.02$, there is an increase in the critical Reynolds number for which the flow becomes unstable. This growth in the value of the critical Reynolds number increases with the volume fraction of the nanoparticles. For the wavenumbers $\alpha = 2$ and $\alpha = 3$, there is a complete stabilization of the flow and the disturbances see their amplitudes being attenuated when the volume fraction of the nanoparticles increases. So the combined effects of the volume fraction of the nanoparticles and the wave number fully stabilize the flow. This result is in good agreement with those of the literature, in particular Turkyilmazoglu [3], Kapen et al. [2]. It appears from this paper that the addition of nanoparticles in the blood increases its inertia blood. The inertia being greater, this attenuates the disturbances and helps to stabilize the flow.

Fig. 4 presents the behavior of Casson's parameter on the evolution of disturbances. In this figure, the amplification rate of the disturbances is represented as a function of the Reynolds number and this for different values of the wave number. For $\alpha = 1$ and $\alpha = 1.02$, we observe for $\beta = 0.5$ and $\beta = 1$ that the flow is completely stable but the amplitude of the disturbances increases when passing from the values $\beta = 0.5$ to $\beta = 1$ which already promises a destabilizing effect of the Casson parameter. For $\beta = 5$ and $\beta = 10$, we observe a certain transition in the flow obviously from stability to instability. Another relevant remark which is observed is that the critical Reynolds number which corresponds to the transitions $\beta = 5$ and $\beta = 10$ decreases when the Casson parameter increases: which confirms the destabilizing effect of this parameter. For $\alpha = 2$ and $\alpha = 3$ the flow is stable but a redistribution of the disturbances is observed when the Casson parameter increases, which undoubtedly makes it possible to affirm that the Casson parameter has a destabilizing effect on the flow. This result is similar to those observed by Ketchate et al. [40]. It appears from this analysis that the non-Newtonian behavior of blood has an effect on its dynamics, so it is very important to take this property of blood into consideration when administering drugs to a patient. Moreover, it appears from this article that taking into account the non-Newtonian behavior of blood offers better results compared to the case where blood is considered as a Newtonian fluid.

Fig. 5 presents the effects of the Buoyancy ration parameter on the stability of the flow. Through this figure, we see that this parameter has an impact on the stability of the flow. For $\alpha = 1$ and $\alpha = 1.02$, the critical Reynolds number for which there is a transition increases when the Buoyancy ratio parameter increases, which means that this parameter has a stabilizing effect. It should be noted that for slightly larger values of the wave number, i.e. $\alpha = 2$ and $\alpha = 3$, no transition is observed and the flow is entirely stable and the buoyancy ratio parameter presents negligible effect on flow stability. The effects of the Richardson number (thermal buoyancy parameter) are presented through Fig. 6. This informs us that the Richardson number has the same effect as the Buoyancy ratio parameter on the stability of the flow. This result is in agreement with those obtained by Mekheimer et al. [26]. It emerges from the present analysis that the Buoyancy forces have an effect on the stability of the blood flow and that their growth decreases the kinetic energy which attenuates the disturbances and contributes to the stability of the flow.

Fig. 7 shows the effects of the chemical reaction through the chemical reaction parameter Kc on the stability of the flow. This figure

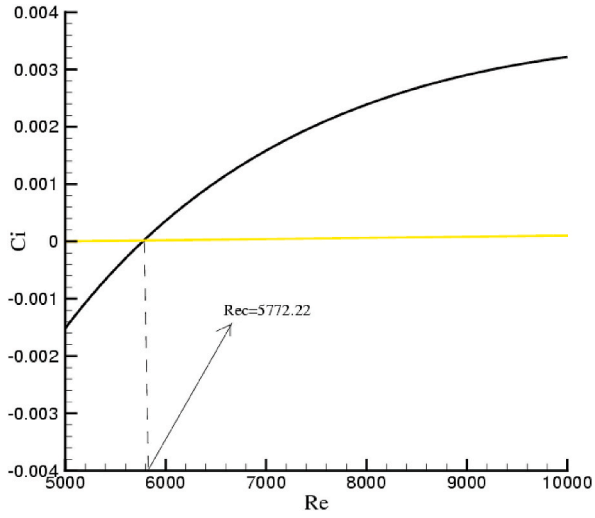

Fig. 2. Perturbation growth rate as a function of Reynolds number.

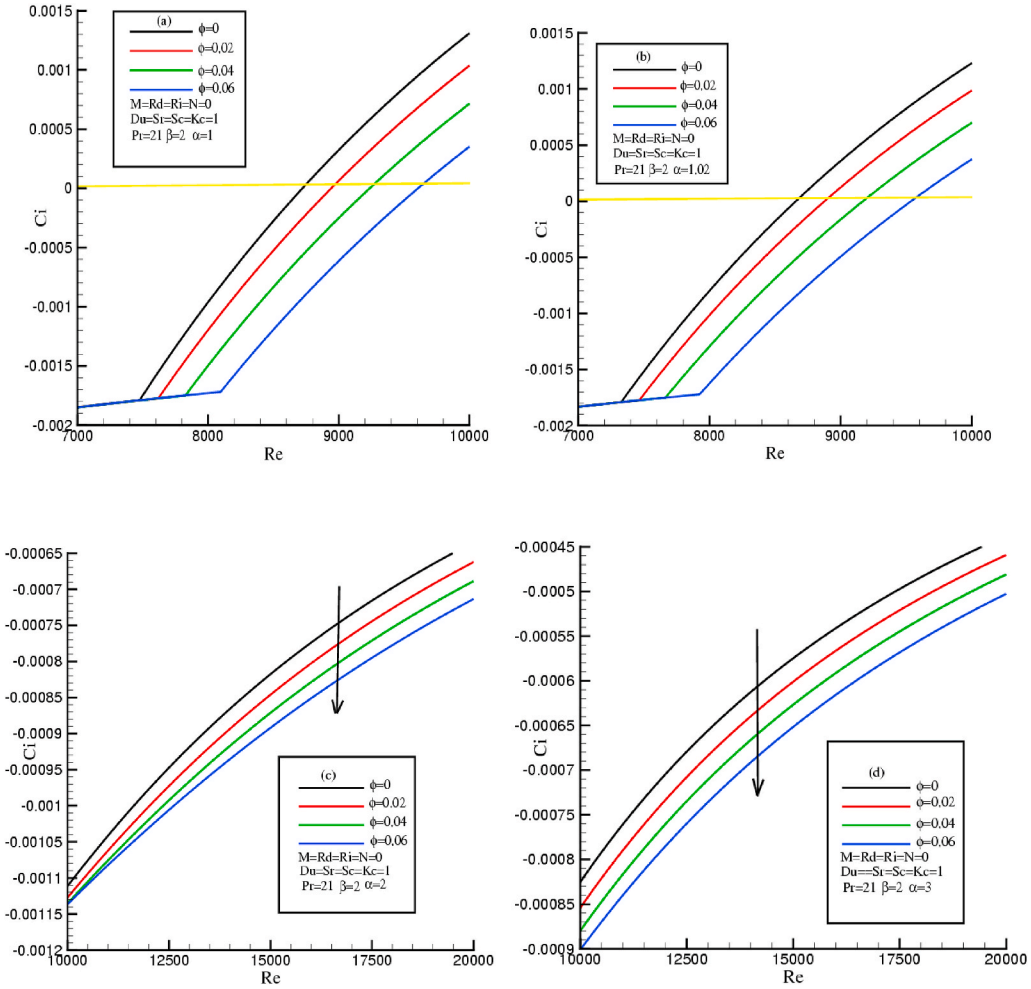

Fig. 3. Effect of volume fraction of nanoparticle on the disturbances Da → ∞,: (a) $\alpha = 1$; (b) $\alpha = 1.02$; (c) $\alpha = 2$; (d) $\alpha = 3$.

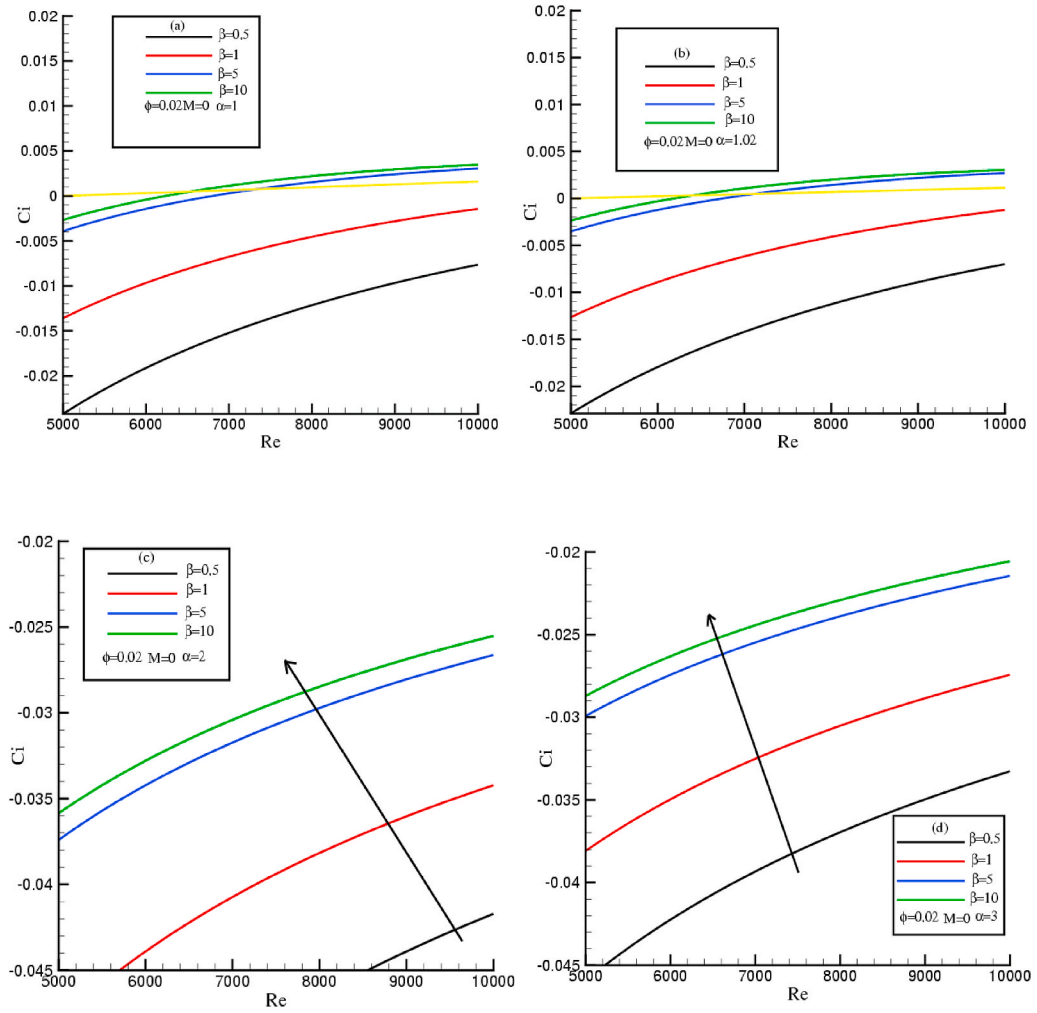

Fig. 4. Effect of Casson parameter on the evolution of disturbance, Da → ∞, Rd = Ri = N = 0, Du = Sr=Kc = 0, Sc = 1, Pr = 21: (a) $\alpha = 1$; (b) $\alpha = 1.02$; (c) $\alpha = 2$; (d) $\alpha = 3$.

informs us that the chemical reaction parameter Kc has a very significant impact. For $\alpha = 1$ and $\alpha = 1.02$, we observe a decrease in the critical Reynolds number when the chemical reaction parameter increases: This justifies a destabilizing character of the chemical reaction parameter Kc. For $\alpha = 2$ and $\alpha = 3$, no transition is observed and there is a superposition of the curves when the parameter Kc increases. This superposition provides the information that the combined effect of the chemical reaction parameter and wave number has negligible effects on the stability of the flow. It appears from this paper that the chemical reactions which are the result of an interaction between the fluid and the magnetic nanoparticles favor the distribution of the disturbances within the flow which maintains the instabilities. Such behavior of the chemical reaction parameter has been observed by authors such as Umavathi and Chamkha [16], and Mekheimer [26].

The effects of thermal radiation on flow stability are shown in Fig. 8. This figure shows that thermal radiation affects flow stability. When the thermal radiation parameter increases, the transition in the flow increases which attenuates the propagation of disturbances in the flow and thus helps in the stabilization of the flow. This stabilizing effect of thermal radiation is of great importance in medicine because it increases the rate of heat transfer from nanoparticles to target areas. This allows the destruction of cancer cells.

The effects of the magnetic field through the Hartmann number are presented in Fig. 9. For $\alpha = 1$ and $\alpha = 1.02$, we observe that in the absence of the magnetic field ($M = 0$), the flow is unstable. In the presence of the magnetic field ($M \neq 0$), the flow is entirely stable. When the Hartmann number increases, an exponential decrease in the amplitude of the disturbances is observed. For $\alpha = 2$ and $\alpha = 3$, the flow is completely stable but the attenuation of disturbances is greater when the wave number increases. So the combined effects of the magnetic field and the wave number further increase the stability field of the flow. We can thus conclude through this analysis that the magnetic field through the Lorentz magnetic force reduces the kinetic energy of the flow which dissipates the disturbances and stabilizes the flow. The stabilizing effects of the magnetic field can be used in biomedical applications to control blood circulation, adjust blood flow during surgical operations, control blood pressure, transport therapeutic agents to a target location in the body and also to the body. With the help of the stabilizing effects of the magnetic field, one can thin the blood.

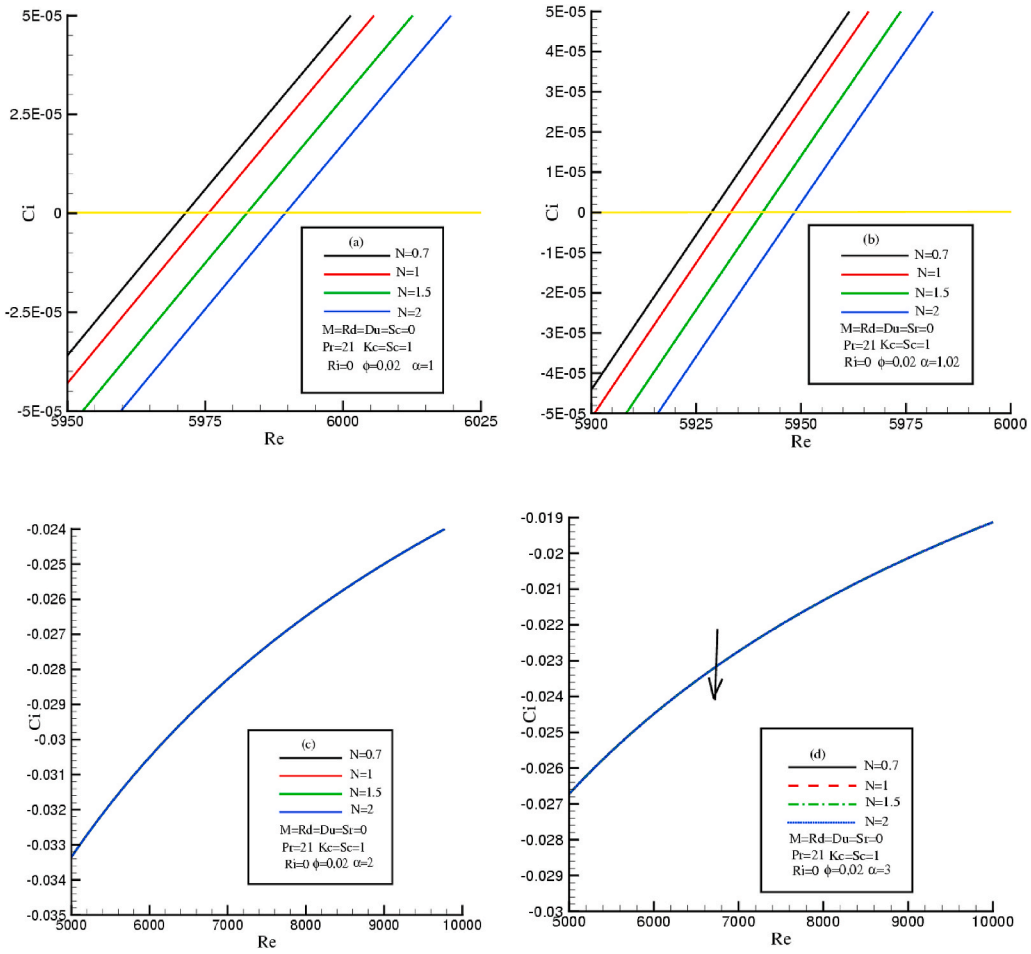

Fig. 5. Effect of buoyancy parameter on the evolution of disturbance, Da → ∞: (a) $\alpha = 1$; (b) $\alpha = 1.02$; (c) $\alpha = 2$; (d) $\alpha = 3$.

Fig. 10 shows the effects of small values of the Darcy number on the stability of the suspension. Through this figure, we see that the amplitude of the disturbances decreases when the Darcy number increases but the flow remains unstable. This allows us to say that the porosity of the medium promises a stabilizing effect on the stability of the flow. To confirm the stabilizing effect of the Darcy number on the stability of the flow, we have presented in Fig. 11 the effects of large values of the Darcy number on the stability of the flow. For Da = 1, the flow always remains unstable. For Da = 10 and Da = 100, two transitions are observed in the flow: a first transition from stability to instability and a second transition which brings the flow back to the stability zone. It is very important to mention that the critical Reynolds number corresponding to the transition increases with the Darcy number. It appears from the present study that the Darcy number contributes to the stability of the flow.

The effects of large values of the Darcy number are presented in Fig. 12. This figure shows a superposition of the curves when the Darcy number goes from Da = 1000 to Da = 10,000. This makes it possible to conclude that the very large values of the Darcy number have negligible effects on the stability of the flow and one has the impression of having a flow in a non-porous medium and the flow model is similar to that studied by Makinde [46]. Our study thus reflects the importance of transporting nanofluids through porous media because in porous media, the exchange surface between the fluid and the nanoparticles is large, which increases the rate of heat transfer. The porosity of the medium also prevents the aggregation of the nanoparticles, which prevents the sedimentation of the nanoparticles.

Figs. 13 and 14 present respectively the effects of Dufour and Soret on the stability of the flow. Through these figures, it is clear that these parameters have a significant impact on the growth rate of disturbances. When the Dufour and Soret numbers increase (Fig. 13a, b, and 14a), we see that the critical Reynolds number for which there is a transition increases. For larger values of the wave number (Fig. 13c, d, 14b) there is stability without transition and the amplitude of the disturbances decreases when these parameters increase. It emerges from this analysis that the Dufour and Soret numbers have a stabilizing effect. Such results are consistent with those obtained by Umavathi and Chamkha [16]. We can thus conclude that the mass transfers induced by the temperature gradients and the heat transfers induced by the concentration gradients within the flow prevent the distribution of the disturbances within the flow which contributes to the stabilization of flow. Thus, the fluid particles located in the zone where the temperature is high have a higher

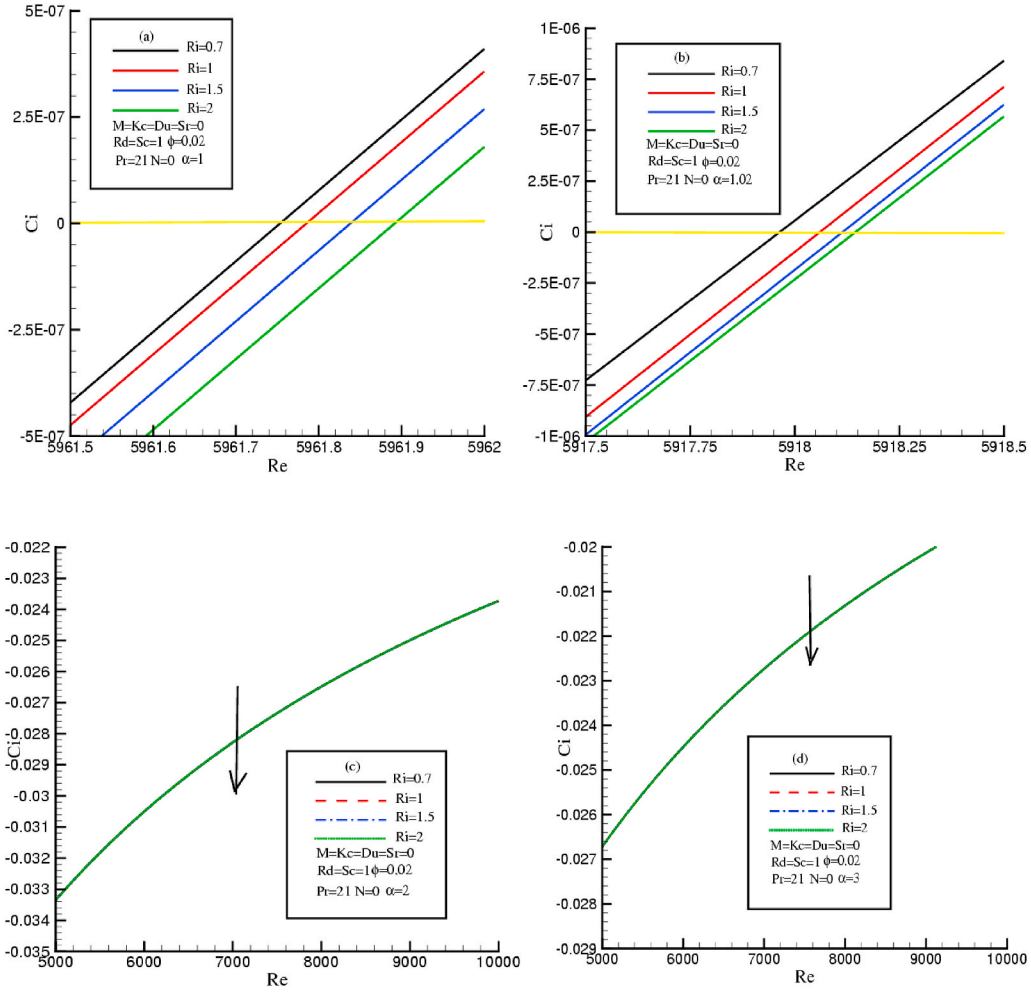

Fig. 6. Effect of Richardson number on the evolution of disturbance, Da → ∞: (a) $\alpha = 1$; (b) $\alpha = 1.02$; (c) $\alpha = 2$; (d) $\alpha = 3$.

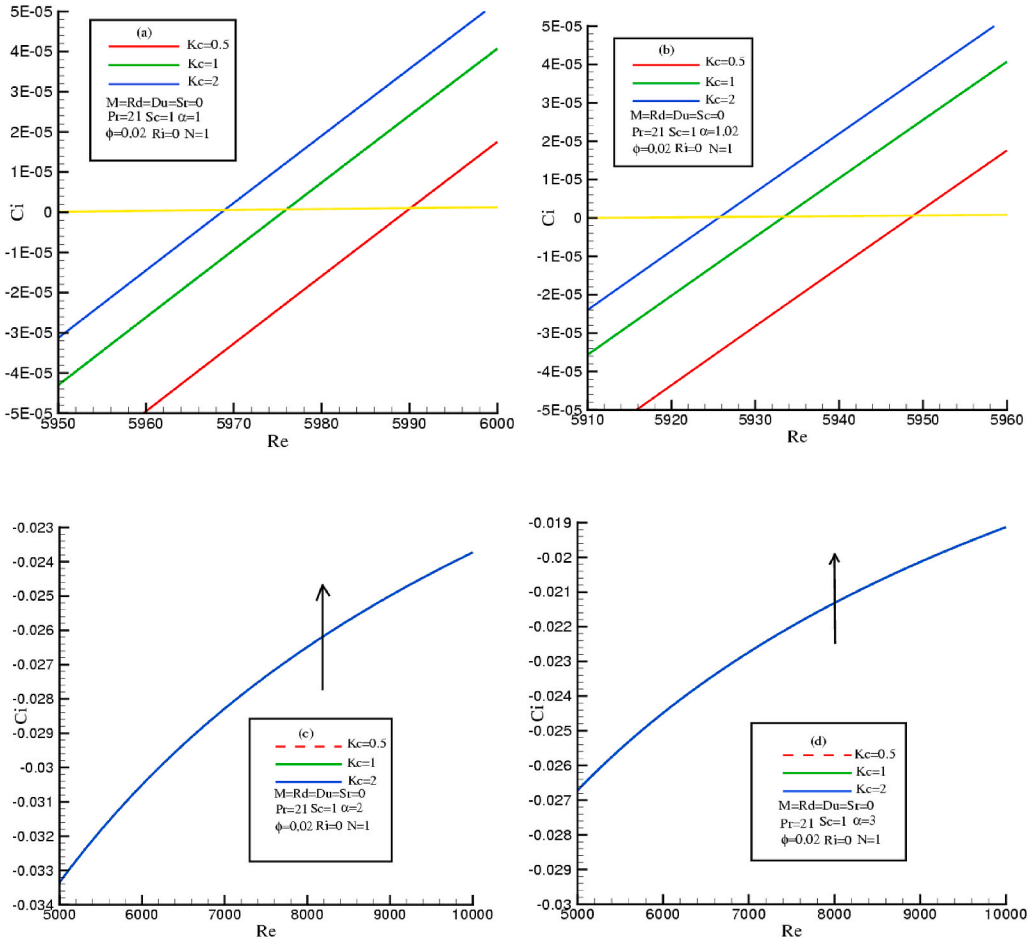

Fig. 7. Effect of chemical reaction parameter on the disturbance evolution, Da → ∞: (a) $\alpha = 1$; (b) $\alpha = 1.02$; (c) $\alpha = 2$; (d) $\alpha = 3$.

energy level, which moves the particles towards the zone of low temperature. Thus, the energy transfer processes are accelerated from the hottest area to the coldest area. This transport process is significant only at the lowest fluid velocities.

6. Conclusion

In this paper, we presented a stability analysis in normal mode of a blood flow treated as Casson's fluid carrying within it magnetic nanoparticles. The study took into account the effects of chemical reaction, mass transfer (Soret effect), energy transfer (Dufour effect), Buoyancy forces, the porosity of the medium, thermal radiation and the magnetic field. The system of eigenvalue equation governing the dynamics was solved by a numerical scheme which exploits the spectral method of collocation. It emerged from the study that the addition of nanoparticles in the blood increased its inertia which helped to stabilize the flow.

The Casson parameter affects the stability of the flow by increasing the amplitude of the disturbances, which reflects its destabilizing effect. It appears from this study that taking into account the non-Newtonian nature of blood is very important when modeling the dynamics of the system because it shows more important and very different results than when blood is treated as a Newtonian fluid. The Darcy number exhibits a stabilizing effect on the flow. It appears from this analysis that the porosity of the medium increases the contact surface between the fluid and the nanoparticles, which increases the rate of heat transfer. The porosity of the medium also prevents the sedimentation of the nanoparticles. Chemical reactions affect flow stability and have a destabilizing effect. It appears from this paper that the reaction between the magnetic nanoparticles and the fluid increases the redistribution of the disturbances within the flow which maintains the instabilities in the flow. The thermal radiation prevents the redistribution of disturbances in the flow, which contributes to the increase in the rate of heat transfer of the nanoparticles in the target areas. The Richardson number, the Buoyancy ratio parameter affect the stability of the flow and contribute to the stability of the flow because they decrease the kinetic energy produced by the flow which prevents the growth of the amplitude of the disturbances and advances the transition in the flow. The Dufour and Soret number contribute to the stability of the flow. We can say that the temperature gradient induced mass transfer effects and the concentration gradient induced heat transfer effects attenuate the amplitude of the disturbances, which delays the transition in the flow. The analysis of the effects of the magnetic field shows that the magnetic field plays a very big role on the stability of the flow.

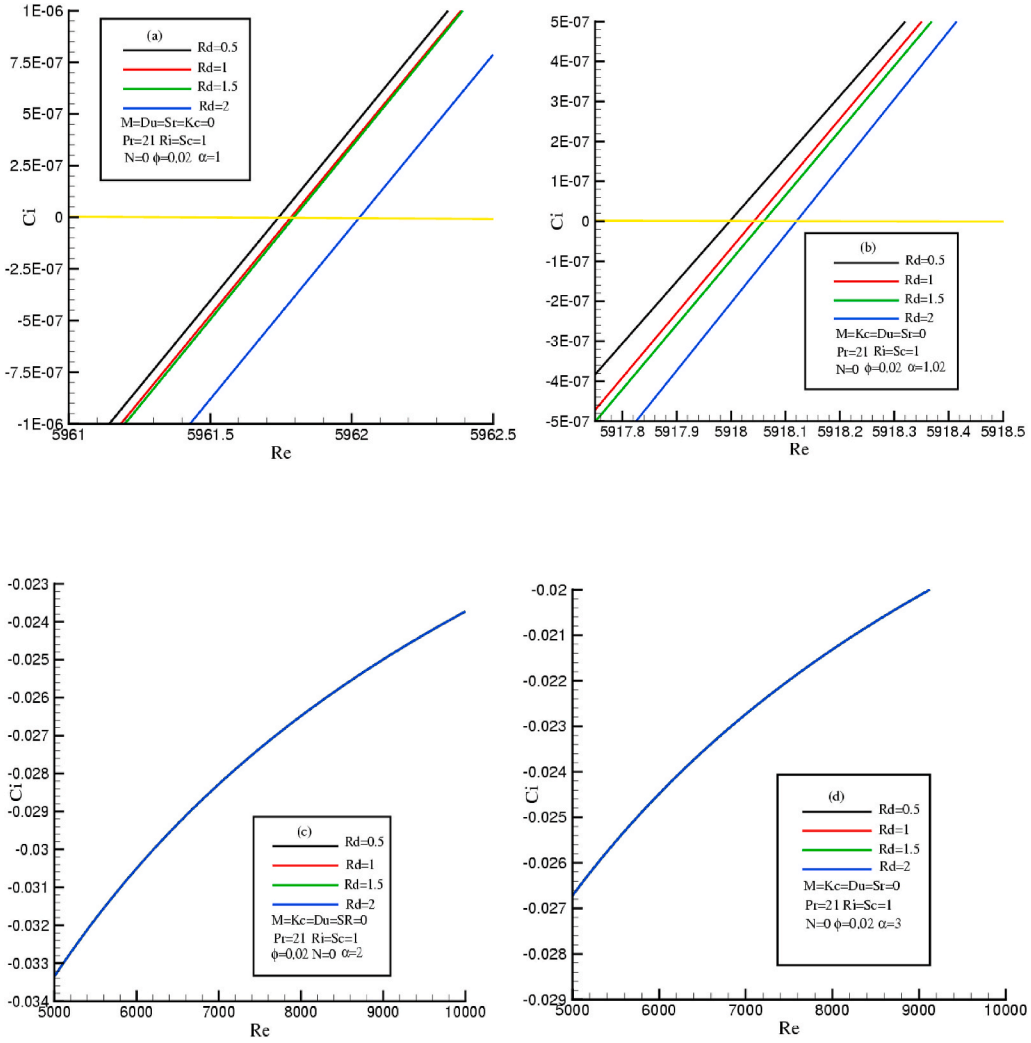

Fig. 8. Effect of thermal radiation on stability of flow, Da → ∞: (a) $\alpha = 1$; (b) $\alpha = 1.02$; (c) $\alpha = 2$; (d) $\alpha = 3$.

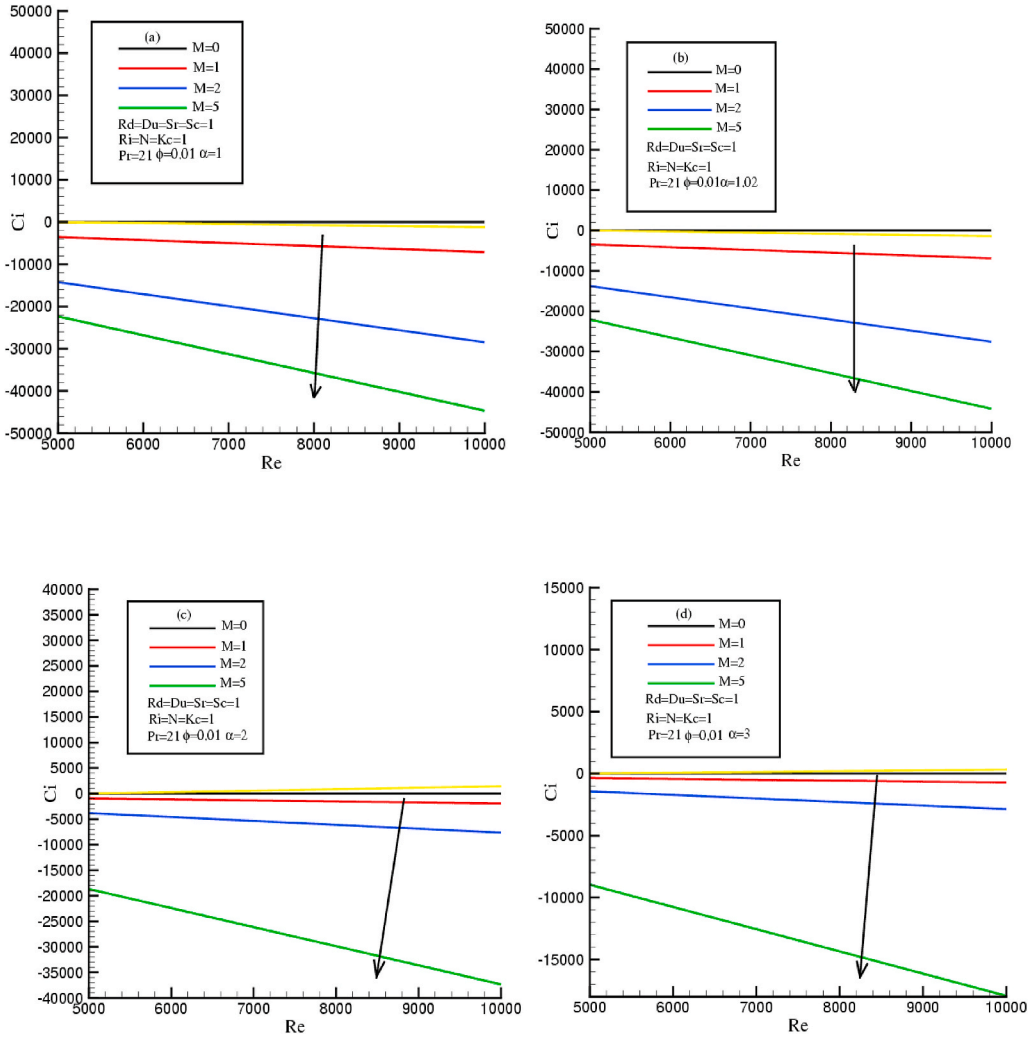

Fig. 9. Effect of Hartmann number on the stability of flow, Da → ∞: (a) $\alpha = 1$; (b) $\alpha = 1.02$; (c) $\alpha = 2$; (d) $\alpha = 3$.

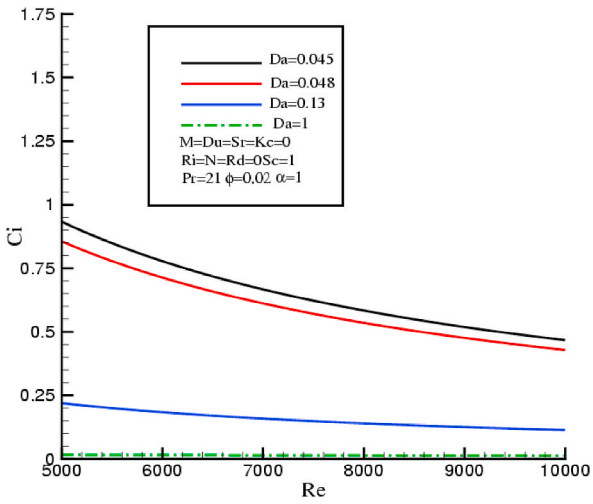

Fig. 10. Effect of small values of Darcy number on the growth of perturbation.

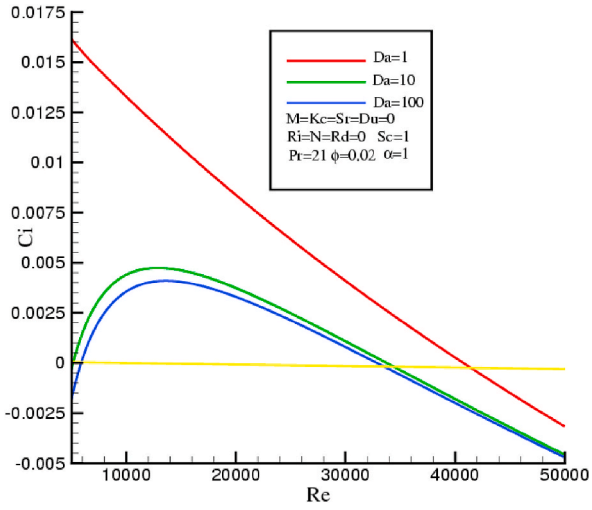

Fig. 11. Effect of large values of Darcy number on the growth of perturbation.

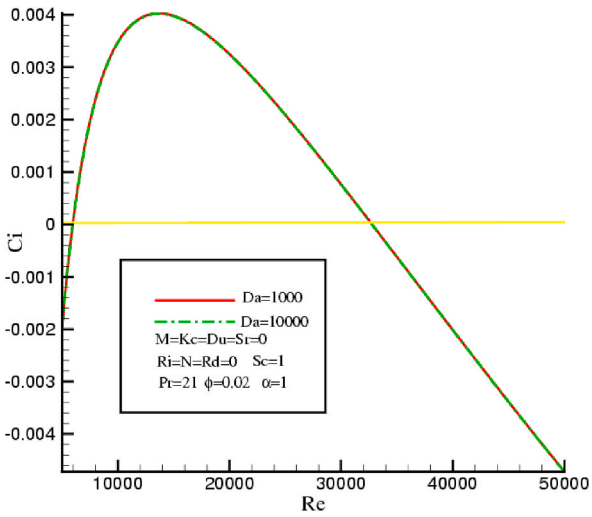

Fig. 12. Effect of very large values of Darcy number on the growth of perturbation.

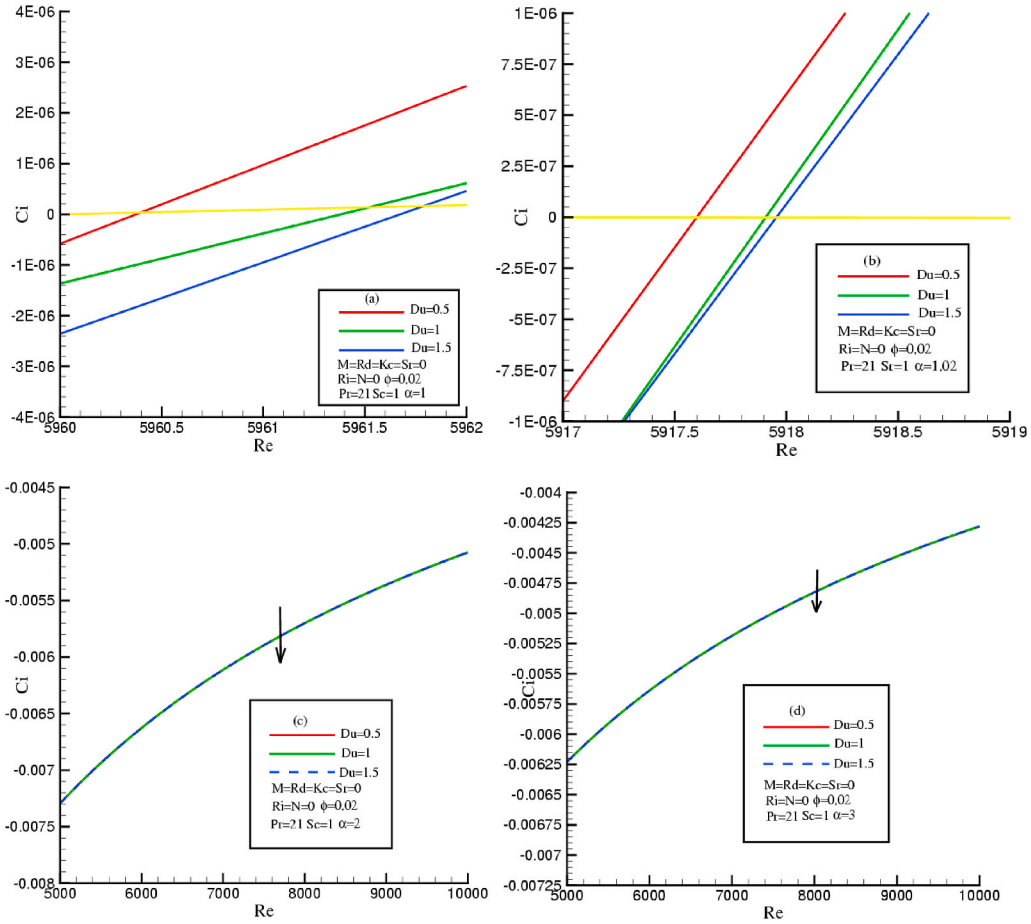

Fig. 13. Effect of Dufour number on the stability of the flow, Da → ∞,: (a) $\alpha = 1$; (b) $\alpha = 1.02$; (c) $\alpha = 2$; (d) $\alpha = 3$.

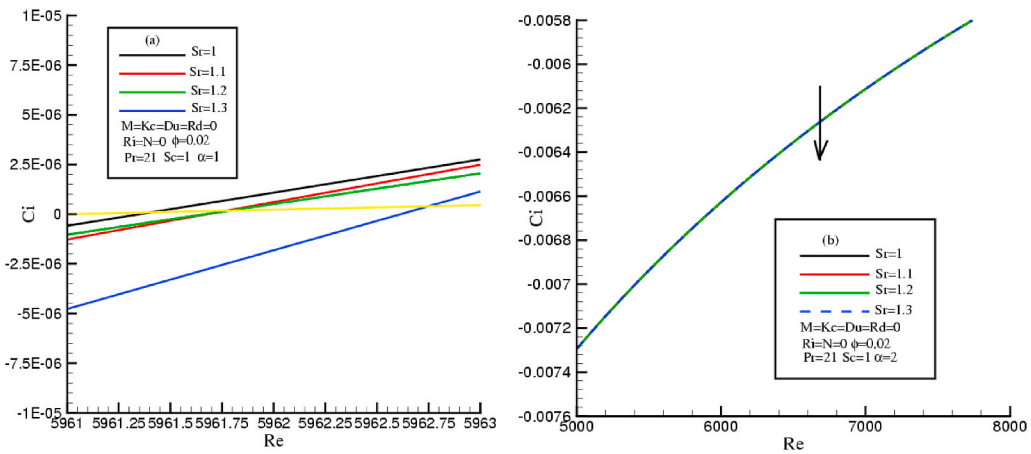

Fig. 14. Effect of Soret number on stability of flow, Da → ∞,: (a) $\alpha = 1$; (b) $\alpha = 2$.

Through the Lorentz force, the magnetic field absorbs the kinetic energy produced by the flow, which dissipates the disturbances and thus stabilizes the flow.

A study taking into consideration the joules effects and the elasticity of the arterial wall may be the subject of future work.

Author contribution statement

Cédric Gervais Njingang Ketchate & Pascalin Tiam Kapen: Conceived and designed the experiments; Performed the experiments; Analyzed and interpreted the data; Contributed reagents, materials, analysis toolsor data; Wrote the paper. Inesse Madiebie-Lambou: Performed the experiments; Analyzed and interpreted the data; Contributed reagents, materials, analysis tools or data. Didier Fokwa, Victorin Chegnimonhan, René Tchinda & Ghislain Tchuen: Analyzed and interpreted the data; Contributed reagents, materials, analysis tools or data.

Funding statement

This research did not receive any specific grant from funding agencies in the public, commercial, or not-for-profit sectors.

Data availability statement

Data will be made available on request.

Declaration competing of interest

The authors declare no competing interests.

References

[1] K.S. Tshivhi, O.D. Makinde, Magneto-nanofluid coolants past heated shrinking/stretching surfaces: dual solutions and stability analysis, Res. Eng. 10 (2021), 100229.
[2] P.T. Kapen, C.G.N. Ketchate, D. Fokwa, G. Tchuen, Linear stability analysis of (Cu-Al2O3)/water hybrid nanofluid flow in porous media in presence of hydromagnetic, small suction and injection effects, Alex. Eng. J. 60 (1) (2021) 1525–1536.
[3] M. Turkyilmazoglu, Single phase nanofluids in fluid mechanics and their hydrodynamic linear stability analysis, Comput. Methods Progr. Biomed. 187 (2020), 105171.
[4] L.A. Lund, Z. Omar, I. Khan, A.H. Seikh, E.S.M. Sherif, K.S. Nisar, Stability analysis and multiple solution of Cu–Al2O3/H2O nanofluid contains hybrid nanomaterials over a shrinking surface in the presence of viscous dissipation, J. Mater. Res. Technol. 9 (1) (2020) 421–432.
[5] P.M. Kumar, K. Palanisamy, V. Vijayan, Stability analysis of heat transfer hybrid/water nanofluids, Mater. Today Proc. 21 (2020) 708–712.
[6] P.T. Kapen, C.G.N. Ketchate, D. Fokwa, G. Tchuen, Instability of hydromagneticCouette flow for hybrid nanofluid through porous media with small suction and injection effects, Int. J. Numer. Methods Heat Fluid Flow 32 (2) (2021) 616–641.
[7] N.A. Zainal, R. Nazar, K. Naganthran, I. Pop, Stability analysis of MHD hybrid nanofluid flow over a stretching/shrinking sheet with quadratic velocity, Alex. Eng. J. 60 (1) (2021) 915–926.
[8] N.S. Ismail, N.M. Arifin, R. Nazar, N. Bachok, Stability analysis of unsteady MHD stagnation point flow and heat transfer over a shrinking sheet in the presence of viscous dissipation, Chin. J. Phys. 57 (2019) 116–126.
[9] N.S. Khashi'ie, N.M. Arifin, R. Nazar, E.H. Hafidzuddin, N. Wahi, I. Pop, Magnetohydrodynamics (MHD) axisymmetric flow and heat transfer of a hybrid nanofluid past a radially permeable stretching/shrinking sheet with Joule heating, Chin. J. Phys. 64 (2020) 251–263.
[10] P.T. Kapen, C.G.N. Ketchate, D. Fokwa, G. Tchuen, Linear stability analysis of non-Newtonian blood flow with magnetic nanoparticles: application to controlled drug delivery, Int. J. Numer. Methods Heat Fluid Flow 27 (2021), 100800.
[11] N.A. Zainal, R. Nazar, K. Naganthran, I. Pop, MHD mixed convection stagnation point flow of a hybrid nanofluid past a vertical flat plate with convective boundary condition, Chin. J. Phys. 66 (2020) 630–644.
[12] H.B. Lanjwani, M.S. Chandio, M.I. Anwar, S.A. Shehzad, M. Izadi, Mhd laminar boundary layer flow of radiative fe-cassonnanofluid: stability analysis of dual solutions, Chin. J. Phys. 76 (2022) 172–186.
[13] M. Jawad, A. Saeed, P. Kumam, Z. Shah, A. Khan, Analysis of boundary layer MHD Darcy-Forchheimer radiative nanofluid flow with soret and dufour effects by means of marangoni convection, Case Stud. Therm. Eng. 23 (2021), 100792.
[14] M. Sheikholeslami, H.R. Kataria, A.S. Mittal, Effect of thermal diffusion and heat-generation on MHD nanofluid flow past an oscillating vertical plate through porous medium, J. Mol. Liq. 257 (2018) 12–25.
[15] N.A. Ahammad, M.V. Krishna, Numerical investigation of chemical reaction, Soret and Dufourimpacts on MHD free convective gyrating flow through a vertical porous channel, Case Stud. Therm. Eng. 28 (2021), 101571.
[16] J.C. Umavathi, A.J. Chamkha, Convective stability of a permeable nanofluid inside a horizontal conduit: fast chemical reactions, Math. Comput. Simulat. 187 (2021) 155–170.
[17] S. Maiti, S. Shaw, G.C. Shit, Fractional order model for thermochemical flow of blood with Dufour and Soret effects under magnetic and vibration environment, Colloids Surf. B Biointerfaces 197 (2021), 111395.
[18] O.A. Bég, V.R. Prasad, B. Vasu, N.B. Reddy, Q. Li, R. Bhargava, Free convection heat and mass transfer from an isothermal sphere to a micropolar regime with Soret/Dufour effects, Int. J. Heat Mass Tran. 54 (1–3) (2011) 9–18.
[19] S.R. Mishra, S. Baag, D.K. Mohapatra, Chemical reaction and Soret effects on hydromagneticmicropolar fluid along a stretching sheet. Engineering Science and Technology, Int. J. 19 (4) (2016) 1919–1928.
[20] A.S. Mittal, Analysis of water-based composite MHD fluid flow using HAM, Int. J. Ambient Energy 42 (13) (2021) 1538–1550.
[21] A. Postelnicu, Heat and mass transfer by natural convection at a stagnation point in a porous medium considering Soret and Dufour effects, Heat Mass Tran. 46 (8) (2010) 831–840.
[22] A.J. Chamkha, A.M. Rashad, Unsteady heat and mass transfer by MHD mixed convection flow from a rotating vertical cone with chemical reaction and Soret and Dufour effects, Can. J. Chem. Eng. 92 (4) (2014) 758–767.
[23] Q. Chen, J. Zhang, X. Zhang, Modeling and measurements of Soret and Dufour effects on the water vapor transfer in membrane-based desiccant solution dehumidification dual-chamber system, Therm. Sci. Eng. Prog. 32 (2022), 101299.

[24] S.R. Sheri, P. Megaraju, M.N. Rajashekar, Impact of Hall Current, Dufour and Soret on transient MHD flow past an inclined porous plate: finite element method, Mater. Today Proc. 59 (2022) 1009–1021.
[25] Q. Chen, J. Zhang, X. Zhang, Modeling and measurements of Soret and Dufour effects on the water vapor transfer in membrane-based desiccant solution dehumidification dual-chamber system, Therm. Sci. Eng. Prog. 32 (2022), 101299.
[26] K.S. Mekheimer, B.M. Shankar, S.F. Ramadan, H.E. Mallik, M.S. Mohamed, On the stability of convection in a non-Newtonian vertical fluid layer in the presence of gold nanoparticles: drug agent for thermotherapy, Mathematics 9 (11) (2021) 1302.
[27] M.V. Krishna, N.A. Ahamad, A.F. Aljohani, Thermal radiation, chemical reaction, Hall and ion slip effects on MHD oscillatory rotating flow of micro-polar liquid, Alex. Eng. J. 60 (3) (2021) 3467–3484.
[28] S.N.A. Salleh, N. Bachok, N.M. Arifin, F.M. Ali, Numerical analysis of boundary layer flow adjacent to a thin needle in nanofluid with the presence of heat source and chemical reaction, Symmetry 11 (4) (2019) 543.
[29] M. Mustafa, J.A. Khan, T. Hayat, A. Alsaedi, Buoyancy effects on the MHD nanofluid flow past a vertical surface with chemical reaction and activation energy, Int. J. Heat Mass Tran. 108 (2017) 1340–1346.
[30] M.V. Krishna, N.A. Ahammad, A.J. Chamkha, Radiative MHD flow of Casson hybrid nanofluid over an infinite exponentially accelerated vertical porous surface, Case Stud. Therm. Eng. 27 (2021), 101229.
[31] N.A. Sheikh, D.L.C. Ching, I. Khan, D. Kumar, K.S. Nisar, A new model of fractional Casson fluid based on generalized Fick's and Fourier's laws together with heat and mass transfer, Alex. Eng. J. 59 (5) (2020) 2865–2876.
[32] G. Rasool, A.J. Chamkha, T. Muhammad, A. Shafiq, I. Khan, Darcy-Forchheimer relation in Casson type MHD nanofluid flow over non-linear stretching surface, Propul. Power Res. 9 (2) (2020) 159–168.
[33] A.S. Kamran, M. Hussain, N. Sagheer, A. Akmal, Numerical study of magnetohydrodynamics flow in Cassonnanofluid combined with Joule heating and slip boundary conditions, Results Phys. 7 (2021) 3037–3048.
[34] S.M. Mousavi, M.N. Rostami, M. Yousefi, S. Dinarvand, I. Pop, M.A. Sheremet, Dual solutions for Casson hybrid nanofluid flow due to a stretching/shrinking sheet: a new combination of theoretical and experimental models, Chin. J. Phys. 71 (2021) 574–588.
[35] A. Hamid, Terrific effects of Ohmic-viscous dissipation on Cassonnanofluid flow over a vertical thin needle: buoyancy assisting and opposing flow, J. Mater. Res. Technol. 9 (5) (2020) 11220–11230.
[36] M.V. Krishna, N.A. Ahamad, A.J. Chamkha, Radiation absorption on MHD convective flow of nanofluids through vertically travelling absorbent plate, Ain Shams Eng. J. 12 (3) (2021) 3043–3056.
[37] C.G.N. Ketchate, P.T. Kapen, D. Fokwa, G. Tchuen, Stability analysis of mixed convection in a porous horizontal channel filled with a Newtonian Al2O3/Water nanofluid in presence of magnetic field and thermal radiation, Chin. J. Phys. 79 (2022) 514–530.
[38] M.G. Sobamowo, Combined effects of thermal radiation and nanoparticles on free convection flow and heat transfer of casson fluid over a vertical plate, Int. J. Chem. Eng. 2018 (2018) 1–25.
[39] S.F. Ahmmed, R. Biswas, M. Afikuzzaman, Unsteady MHD free convection flow of nano fluid through an exponentially accelerated inclined plate embedded in a porous medium with variable thermal conductivity in the presence of radiation, J. Nano fluids. 7 (5) (2018) 891–901.
[40] C.G.N. Ketchate, P.T. Kapen, D. Fokwa, G. Tchuen, Stability analysis of non-Newtonian blood flow conveying hybrid magnetic nanoparticles as target drug delivery in presence of inclined magnetic field and thermal radiation: application to therapy of cancer, Inform. Med. Unlocked 27 (2021), 100800.
[41] F. Mabood, A.T. Akinshilo, Stability analysis and heat transfer of hybrid Cu-Al2O3/H2O nanofluids transport over a stretching surface, Int. Commun. Heat Mass Tran. 123 (2021), 105215.
[42] A. urRehman, Z. Abbas, Stability analysis of heat transfer in nanomaterial flow of boundary layer towards a shrinking surface: hybrid nanofluid versus nanofluid, Alex. Eng. J. 61 (12) (2022) 10757–10768.
[43] M. Sheikholeslami, D.D. Ganji, M.Y. Javed, R. Ellahi, Effect of thermal radiation on magnetohydrodynamicsnanofluid flow and heat transfer by means of two phase model, J. Magn. Magn Mater. 374 (2015) 36–43.
[44] S.A. Bakar, N.M. Arifin, N. Bachok, F.M. Ali, Effect of thermal radiation and MHD on hybrid Ag–TiO2/H2O nanofluid past a permeable porous medium with heat generation, Case Stud. Therm. Eng. 28 (2021), 101681.
[45] B.M. Shankar, I.S. Shivakumara, Magnetohydrodynamic stability of pressure-driven flow in an anisotropic porous channel: accurate solution, Appl. Math. Comput. 321 (2018) 752–767.
[46] O.D. Makinde, Chebyshev collocation approach to stability of blood flows in a large artery, Afr. J. Biotechnol. 11 (41) (2012) 9881–9887.